

Article

Assessing the Contribution of the Neutral Blocks in DNA/Block-Copolymer Polyplexes: Poly(acrylamide) vs. Poly(ethylene Oxide)

Renata Mello Giona^{1,2}, Leticia Vitorazi^{2,3} and Watson Loh^{2,*} 

¹ LaMaFI—Laboratório de Materiais e Fenômenos de Interface, Chemistry Department, Universidade Tecnológica Federal do Paraná (UTFPR), Medianeira, Curitiba 85884-000, Paraná (PR), Brazil

² Institute of Chemistry, Universidade Estadual de Campinas (UNICAMP), Caixa Postal 6154, Campinas 13083-970, São Paulo State (SP), Brazil

³ Laboratório de Materiais Poliméricos, EEIMVR, Universidade Federal Fluminense, Volta Redonda 27255-125, Rio de Janeiro (RJ), Brazil

* Correspondence: wloh@unicamp.br

Abstract: The interaction of DNA with different block copolymers, namely poly (trimethylammonium chloride methacryloyloxy)ethyl)-block-poly(acrylamide), i.e., (PTEA)-*b*-(PAm), and poly (trimethylammonium chloride methacryloyloxy)ethyl)-block-poly(ethylene oxide), i.e., (PTEA)-*b*-(PEO), was studied. The nature of the cationic block was maintained fixed (PTEA), whereas the neutral blocks contained varying amounts of acrylamide or (ethylene oxide) units. According to results from isothermal titration microcalorimetry measurements, the copolymers interaction with DNA is endothermic with an enthalpy around 4.0 kJ mol⁻¹ of charges for (PTEA)-*b*-(PAm) and 5.5 kJ mol⁻¹ of charges for (PTEA)-*b*-(PEO). The hydrodynamic diameters of (PTEA)-*b*-(PEO)/DNA and (PTEA)-*b*-(PAm)/DNA polyplexes prepared by titration were around 200 nm at charge ratio ($Z_{+/-}$) < 1. At $Z_{+/-}$ close and above 1, the (PTEA)₅₀-*b*-(PAm)₅₀/DNA and (PTEA)₅₀-*b*-(PAm)₂₀₀/DNA polyplexes precipitated. Interestingly, (PTEA)₅₀-*b*-(PAm)₁₀₀₀/DNA polyplexes remained with a size of around 300 nm even after charge neutralization, probably due to the size of the neutral block. Conversely, for (PTEA)₉₆-*b*-(PEO)₁₀₀/DNA polyplexes, the size distribution was broad, indicating a more heterogeneous system. Polyplexes were also prepared by direct mixture at $Z_{+/-}$ of 2.0, and they displayed diameters around 120–150 nm, remaining stable for more than 10 days. Direct and reverse titration experiments showed that the order of addition affects both the size and charge of the resulting polyplexes.

Keywords: polyplex; coacervation; DNA; block copolymers; ITC; polyelectrolytes



Citation: Giona, R.M.; Vitorazi, L.; Loh, W. Assessing the Contribution of the Neutral Blocks in DNA/Block-Copolymer Polyplexes: Poly(acrylamide) vs. Poly(ethylene Oxide). *Molecules* **2023**, *28*, 398. <https://doi.org/10.3390/molecules28010398>

Academic Editors: Artur J.M. Valente, Mariette M. Pereira and Alberto Pais

Received: 8 December 2022

Revised: 24 December 2022

Accepted: 26 December 2022

Published: 3 January 2023



Copyright: © 2023 by the authors. Licensee MDPI, Basel, Switzerland. This article is an open access article distributed under the terms and conditions of the Creative Commons Attribution (CC BY) license (<https://creativecommons.org/licenses/by/4.0/>).

1. Introduction

Polyelectrolyte self-assemblies are present in many biological systems, and it is interesting to develop artificial self-assemblies that mimic naturally occurring assembly structures [1,2]. For instance, DNA is a highly negatively charged polyelectrolyte and therefore adopts an extended coil conformation in dilute solutions [3,4]. Considering that several diseases can be treated using gene therapy, numerous efforts have been applied to develop efficient DNA delivery vectors. Viruses can transport genetic material into the nucleus once they go through endocytosis to the cell. However, although cationic non-viral vectors are in general more cytotoxic and less efficient, due to safety reasons, there is an increased interest in the development of nonviral vectors using cationic agents [5], for instance, the surfactants CTAB [6], DODAB and DODAC [7], ester-based cationic gemini surfactants [8], and synthetic polymers such as poly(ethyleneimine) [9–11], polylysine [12,13], poly(glycoamidoamine) [14], poly(amide triazole) [15] and poly(amido amine) dendrimer, PAMAM [16–18]. Furthermore, there are current human clinical trials using DNA-based vaccines that target various types of diseases such as autoimmune infectious and against

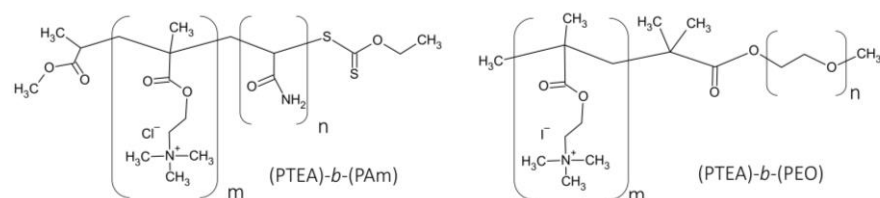
coronavirus, for example [19]. Therefore, it is of great interest to develop carrier materials to improve the systemic release of DNA in the body [19].

Cationic molecules bind to the negatively charged DNA backbone, forming a complex in which the DNA backbone is compacted [20–22]. Several functional groups are interesting to investigate regarding their attachment to macromolecules, such as trimethylammonium [4] and guanidinium [23], among others. In fact, ammonium groups play an important role in the efficiency of genetic material transport with cationic polymers because they form condensed particles with DNA, sometimes referred to as polyplexes [24].

Many studies seek to design and select appropriate DNA carriers and aim at elucidating the features that govern the interaction between the DNA and the cationic agent and how the biological activity of these polyplexes is preserved. Chen and co-workers synthesized a triblock copolymer of polylysine-*b*-polyleucine-*b*-polylysine with different block lengths as free cationic chains and used natural protamine to condense DNA, with results showing that these triblock copolypeptides are able to increase the gene transfection efficiency by a factor of approximately 10^4 times compared with the use of the polyplexes without the free cationic chains [22]. Jung and co-workers prepared several block copolymers in which the cationic block was fixed as poly(N-(2-aminoethyl) methacrylamide) (PAEMA) with varying hydrophilic blocks including poly(ethylene glycol), poly(oligo(ethylene glycol) methyl ether methacrylate), and poly(2-deoxy-2-methacrylamido glucopyranose). According to their results, the nature of the hydrophilic block plays an important role in determining the structures of pDNA–diblock complexes [25]. However, despite the large number of studies involving the interaction of DNA with cationic polyelectrolytes [3,12,21–34], the thermodynamics of the polyplexes formation is not completely understood yet, especially concerning contributions from interaction forces other than electrostatic ones.

Interactions between macromolecules have been extensively characterized by isothermal titration calorimetry (ITC), a technique that enables the direct measurement of the heat exchange involved when one species is titrated into another, providing information on the extent of interaction as well as on enthalpy changes associated with the binding process. Therefore, ITC is an outstanding tool not only to monitor binding processes but also to produce a complete thermodynamic profile of the system [35–37].

In this paper, we report the preparation of three different block copolymers containing the same cationic and neutral portions but with different neutral block lengths, namely (trimethylammonium chloride methacryloyl-*oxyethyl*)-block-poly(acrylamide), (PTEA)₅₀-*b*-(PAm)₅₀, and (PTEA)₅₀-*b*-(PAm)₂₀₀ and (PTEA)₅₀-*b*-(PAm)₁₀₀₀. Another copolymer containing poly(ethylene oxide) as the neutral block, (PTEA)₉₆-*b*-(PEO)₁₀₀, was also used, as shown in Scheme 1. In this approach, the block copolymers used contained the same cationic block, allowing the assessment of the influence of the type and size of their neutral blocks on the formation of DNA polyplexes. These polyplexes were characterized by isothermal titration microcalorimetry (ITC), zeta potential and dynamic light-scattering measurements, and via circular dichroism spectroscopy.



Scheme 1. Chemical structures of block copolymers used in this study: (PTEA)₅₀-*b*-(PAm)₅₀, (PTEA)₅₀-*b*-(PAm)₂₀₀, (PTEA)₅₀-*b*-(PAm)₁₀₀₀, and (PTEA)₉₆-*b*-(PEO)₁₀₀.

2. Results and Discussion

Three block copolymers were synthesized with varying sizes of their polyacrylamide blocks and with the same cationic block. The intent was to verify the influence of their neutral acrylamide blocks on the stabilization of the complex formed through the interaction

between the cationic portion of the copolymer and the negatively charged DNA. In addition, another block copolymer was modified to contain the same cationic block and with a PEO neutral block instead of PAm, namely (PTEA)₉₆-*b*-(PEO)₁₀₀. Table 1 summarizes the copolymers prepared as well as the expected size of each block considering the quantity of reactants used in the synthesis of (PTEA)-*b*-(PAm). Their dispersity values (M_w/M_n) were calculated using GPC experimental data. The copolymer (PDMAEMA)₉₆-*b*-(PEO)₁₀₀ was modified in order to obtain the block copolymer (PTEA)₉₆-*b*-(PEO)₁₀₀, and its composition was provided by the supplier.

Table 1. Composition of the copolymers studied.

	Number of Monomers of Cationic Block	M_w , Cationic Block (g mol ⁻¹)	Number of Monomers of Neutral block	M_w , Neutral Block (g mol ⁻¹)	Dispersity (M_w/M_n)
(PTEA) ₅₀ - <i>b</i> -(PAm) ₅₀	50	10,581	50	3550	1.5 *
(PTEA) ₅₀ - <i>b</i> -(PAm) ₂₀₀	50	10,203	200	14,200	1.9 *
(PTEA) ₅₀ - <i>b</i> -(PAm) ₁₀₀₀	50	10,526	1000	71,000	2.3 *
(PDMAEMA) ₉₆ - <i>b</i> -(PEO) ₁₀₀	96	15,000	113	5000	1.3 **
(PTEA) ₉₆ - <i>b</i> -(PEO) ₁₀₀	96	28,695	113	5000	1.3 **

* Experimental values obtained as described in the supplementary material. ** According to the copolymer provider.

The interaction of copolymers with DNA was investigated using ITC, DLS, zeta potential, and circular dichroism measurements, varying the charge ratio between polymer and DNA ($Z_{+/-}$ ratio), that is, the ratio between number of positive charge equivalents of the polymer and the negative charge equivalents of the nucleic acid. We decided to work in low-ionic-strength media because the presence of electrolytes might increase the size of polyplexes due to charge screening effects [38].

Calorimetric titrations of DNA solutions with (PTEA)-*b*-(PAm) were performed to investigate the energetics of binding. Figure 1a–c show the integrated heats of reaction plotted against $Z_{+/-}$. For the addition of (PTEA)-*b*-(PAm) to DNA, in the presence of NaCl 5.0 mM, the enthalpy of interaction (ΔH) is around 4.0 kJ mol⁻¹ expressed per mole of added copolymer in each injection and is constant and endothermic up to $Z_{+/-}$ value around 0.85. This means that this complex formation is entropically driven, probably due to the release of water molecules and counterions that occurs when the opposite charged chains bind. The order of magnitude of these enthalpy changes agrees with previous determination for the interaction of other oppositely charged polymers, suggesting a general behavior [7,38]. Similarly, for (PTEA)₉₆-*b*-(PEO)₁₀₀, ITC experiments showed that the interaction is also endothermic with larger values of enthalpy of binding (ΔH) around 5.5 kJ mol⁻¹ expressed per mole of added copolymer in each injection when compared to the (PTEA)-*b*-(PAm) copolymers and that it remains constant up to $Z_{+/-}$ of 0.83 (Figure 1d).

In mixtures with $Z_{+/-}$ below 1.0, DNA in excess interacts with the complexes to produce negatively charged and kinetically stable aggregates. Subsequently to the abrupt decrease in ΔH , after charge neutralization, as $Z_{+/-}$ increases, the observation of ΔH values close to zero indicates that the added polycation does not interact with the structures formed [38]. As soon as a charge ratio of around 1.0 is reached, and before ΔH is close to zero and constant, an endothermic peak occurs. Previous results reported that as the charge ratio approaches stoichiometry, the repulsion decreases, and the complexes gradually transform into a larger complex coacervate by stepwise aggregation until nanophase separation [39]. These findings corroborate with the previously proposed two-step process, in which the first process is related to the formation of complexes of highly charged polyelectrolyte of size around 100 nm, and the second process is the transition of a coacervate phase [38,40]. On the other hand, the complexation between quaternized poly(2-(dimethylamino)ethyl methacrylate)-*b*-laurylmethacrylate-*b*-(oligo ethylene glycol) methacrylate amphiphilic triblock terpolymer micelles follows a two-step interaction process only for the terpolymer/short DNA micellar polyplexes (113 bp), and a only a single process is observed when complexation occurs with the 2000 bp DNA [41].

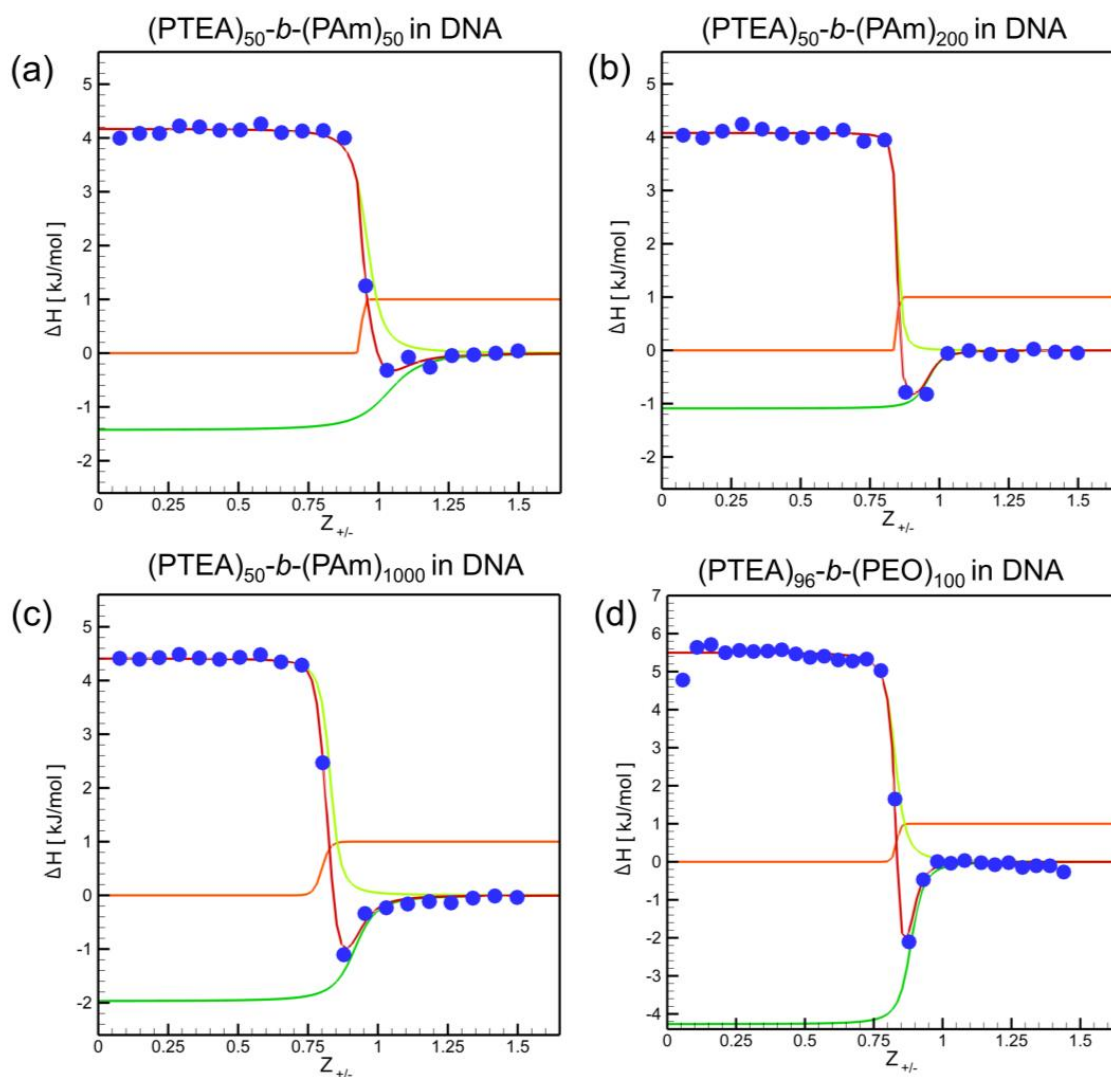


Figure 1. Binding enthalpy for titration (a) PTEA₅₀-b-PAm₅₀, (b) PTEA₅₀-b-PAm₂₀₀, (c) PTEA₅₀-b-PAm₁₀₀₀, and (d) PTEA₉₆-b-PEO₁₀₀ with DNA, as a function of their charge ratios ($Z_{+/-}$).

These curves (Figure 1) display features already reported for other electrostatic binding processes involving surfactants and polymers, such as the positive values for enthalpy of binding and the appearance of a bump in the ITC curves close to charge neutrality [38,40]. The latter feature has been ascribed to a two-stage association process in which ion pairs are formed initially, and closer to charge neutrality, the whole system rearranges to form a coacervate that eventually phase separates. In order to better understand the association thermodynamics in the two processes, A and C, observed (with A standing for aggregation and C coacervation), fitting of the calorimetry data was performed using the modified version of the Multiple Non-Interacting Sites (MNIS) model as previously proposed [38]. The interaction between both macromolecules is associated with a binding enthalpy (ΔH_b), a binding constant K_b , and a reaction stoichiometry n , which is the number of binding sites assuming that they do not interact one with another [38]. As one macromolecule is titrated into the other, the heat exchange is quantified by the derivative of the heat related to the incremental addition of a small amount of macromolecule (ligand). Thus, using the

charge ratio $Z_{+/-}$ to associate the concentration of both macromolecules, the enthalpy can be defined by Equation (1):

$$\Delta H(Z, n, r) = \frac{1}{2} \Delta H_b \left(1 + \frac{n - Z - r}{\sqrt{(n + Z + r)^2 - 4Zn}} \right) \quad (1)$$

where $r = 1/K_b[M]$, and $[M]$ is the molar concentration of the macromolecule in the cell. To account for the two-step titration, one assumes that the heat exchange is the sum of the two contributions, $\Delta H_A(Z, n_A, r_A)$ for the polyplexes binding and $\Delta H_C(Z, n_C, r_C)$ for the coacervation, where A stands for aggregates and C for coacervates formation. Thus, the total enthalpy change for the titration is the sum of the binding enthalpies for each process, ΔH_b^A and ΔH_b^C , namely aggregation and coacervation, respectively, expressed as:

$$\Delta H(Z) = \Delta H_A(Z, n_A, r_A) + \alpha(Z) \Delta H_C(Z, n_C, r_C), \quad (2)$$

where the function $\alpha(Z)$ is the fraction of the coacervate phase formed at a specific charge ratio $Z_{+/-}$ and defined as follows:

$$\alpha(Z) = \left(1 + \exp\left(-\frac{(Z - Z_0)}{\sigma}\right) \right)^{-1}, \quad (3)$$

From the binding enthalpy (ΔH_b), the stoichiometry (n), and the binding constant (K_b), the changes in free energy (ΔG) and in entropy (ΔS) of the interaction can be calculated as follows:

$$\Delta G = -RT \ln K_b, \quad (4)$$

$$\Delta S = \frac{(\Delta H_b - \Delta G)}{T}, \quad (5)$$

These parameters were obtained considering the molar composition in terms of charge equivalents (for this system, one charge equals one mer). Table 2 presents the thermodynamic parameters obtained by the fitting of the ITC curves for processes A and C, as described above.

Table 2. Thermodynamic parameters obtained by fitting of the ITC curves for processes A and C.

Process A	ΔH_b^A (kJ mol ⁻¹)	K_b	n_A	ΔG (kJ mol ⁻¹)	ΔS (J mol ⁻¹ K ⁻¹)
PTEA ₅₀ - <i>b</i> -PAm ₅₀ in DNA	4.2	3.1×10^6	0.96	-37.0	138
PTEA ₅₀ - <i>b</i> -PAm ₂₀₀ in DNA	4.1	2.5×10^7	0.85	-42.2	155
PTEA ₅₀ - <i>b</i> -PAm ₁₀₀₀ in DNA	4.4	6.3×10^6	0.83	-38.8	145
PTEA ₉₆ - <i>b</i> -PEO ₁₀₀ in DNA	5.5	5.0×10^6	0.83	-38.2	147
Process C	ΔH_b^C (kJ mol ⁻¹)	K_b	n_C	ΔG (kJ mol ⁻¹)	ΔS (J mol ⁻¹ K ⁻¹)
PTEA ₅₀ - <i>b</i> -PAm ₅₀ in DNA	-1.4	6.6×10^5	1.04	-33.2	107
PTEA ₅₀ - <i>b</i> -PAm ₂₀₀ in DNA	-1.1	3.1×10^6	0.96	-37.1	121
PTEA ₅₀ - <i>b</i> -PAm ₁₀₀₀ in DNA	-2.0	1.4×10^6	0.92	-35.1	111
PTEA ₉₆ - <i>b</i> -PEO ₁₀₀ in DNA	-4.3	1.4×10^6	0.89	-35.0	103

* The parameters were obtained considering the molar composition in terms of charge equivalents (for this system, one charge equals one mer).

Further analysis of the thermodynamics of process C shows that the coacervation/precipitation is exothermic for the addition of all the block copolymers in DNA. The enthalpy values were similar for all the polyplexes, with exception of PTEA₉₆-*b*-PEO₁₀₀ with DNA, whose binding is found to be more energetic.

Moreover, the entropy changes are positive and in the range of 103–155 J mol⁻¹ K⁻¹, confirming an entropically driven process because enthalpy values are positive, which is in accordance with previous studies [38,42]. The entropy values of process A are greater than those of process C, as is for Gibbs free energy. In addition, the enthalpy values that were positive in process A became negative in process C although both processes are controlled

by entropy. Process A occurs in a stoichiometry below that of process B, with the first continuing up to $Z = 0.83$ – 0.96 , while the second occurs at $Z = 0.89$ – 1.04 , suggesting that coacervation only takes place when most of the charges are neutralized. With respect to K , the values obtained in the present study are larger than values reported in previous studies [43].

In order to shed light on the structural changes upon the different complexation processes, a DLS investigation was performed and compared with the calorimetry data as in Figure 2a–d, where I displays the calorimetric data presented above, II is the scattering intensity data, III the hydrodynamic diameters with polydispersity index values, and IV shows the zeta potential data.

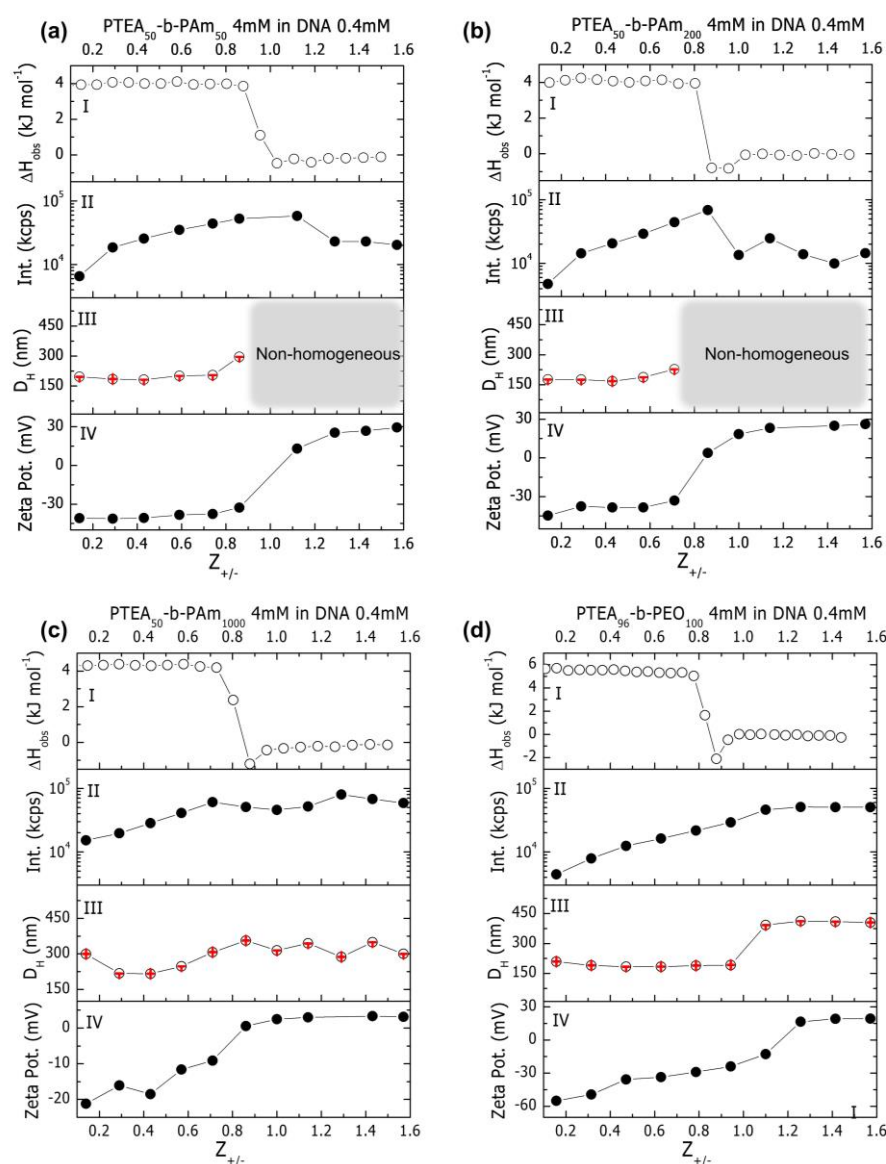


Figure 2. Comparison of ITC data with DLS results: intensity of scattering; hydrodynamic diameter ($Z_{average}$) with PDI values indicated as red bars; and zeta potential values for titration of DNA with (PTEA)₅₀-b-(PAm)₅₀ (a), (PTEA)₅₀-b-(PAm)₂₀₀ (b), (PTEA)₅₀-b-(PAm)₁₀₀₀ (c), and (PTEA)₉₆-b-(PEO)₁₀₀ (d).

The scattering intensity data show that there is an increase in scattering intensity with an increase in the charge ratio up to the value of $Z_{+/-}$ around 0.8. Then, there is a slight decrease in scattering intensity for polymers with PAm₅₀ and PAm₂₀₀ blocks for higher charge ratios. This behavior is different for the system composed by PAm₁₀₀₀, where these values remain somewhat constant for intermediate $Z_{+/-}$ values with a slight increase trend.

Studies show that this variation in intensity is a typical feature associated with the formation of coacervates or precipitates during these titrations; when the intensity decreases after coacervation or precipitation, this indicates that larger aggregates are formed that phase separate from the solution and stop scattering light [38].

The DLS data show that the size of the aggregates is around 200 nm and that after charge neutralization, precipitation occurs for the polymers containing the shorter blocks, PAm₅₀ and PAm₂₀₀. Interestingly, the same was not observed for the copolymers (PTEA)₅₀-*b*-(PAm)₁₀₀₀ and (PTEA)₉₆-*b*-(PEO)₁₀₀/DNA. In fact, as illustrated in Figure 3e, the diameter of (PTEA)₉₆-*b*-(PEO)₁₀₀/DNA and (PTEA)₅₀-*b*-(PAm)₁₀₀₀/DNA polyplexes is around 200 nm at $Z_{+/-} = 0.6$, and even at $Z_{+/-} = 2.0$, after charge neutralization, (PTEA)₅₀-*b*-(PAm)₁₀₀₀/DNA polyplexes remained with finite size, only slightly larger, possibly due to the larger size of their neutral blocks that prevented their growth and precipitation. Similarly, for (PTEA)₉₆-*b*-(PEO)₁₀₀/DNA, the complexes also presented finite sizes although their size distribution was broader, indicating that possibly some polyplexes coacervated; but still, the aggregates remained with size in the order of 10² nm, shedding light on the effect of a larger neutral block on the aggregate's size. For (PTEA)₅₀-*b*-(PAm)₅₀/DNA and (PTEA)₅₀-*b*-(PAm)₂₀₀/DNA polyplexes, at $Z_{+/-} = 0.6$, their diameter was also around 200 nm, but at $Z_{+/-} = 2.0$, precipitation was observed. These results show that the size of the neutral block plays an essential role in determining the size of the polyplexes and the extent of coacervation/precipitation, as, for instance, the longer polyacrylamide block of (PTEA)₅₀-*b*-(PAm)₁₀₀₀ was able to prevent its polyplex from precipitating. Figure 3 schematically illustrates the mechanism envisaged for the formation of polyplexes depending on the size and nature of their neutral blocks: the short polyacrylamide blocks eventually precipitate, whereas increasing the polyacrylamide block, the coacervates maintain almost the same size even after charge neutralization. When PEO is the neutral block, even with only 100 PEO units, finite sized coacervates are observed as remaining after charge neutralization, showing that this neutral block is more efficient in preventing the formation of precipitate.

Zeta potential data (Figure 2-IV) for titration of copolymers in DNA show the formation of negatively charged aggregates with zeta potential values around -45 mV for charge ratios up to $Z_{+/-} \sim 0.8$ for systems containing PAm₅₀ (Figure 2a) and PAm₂₀₀ (Figure 2b). Above that, charge inversion occurs in the range of $Z_{+/-}$ 0.9 and 1, respectively. Differently, for the polymer PAm₁₀₀₀ (Figure 2c), these aggregates remain with small negative zeta potentials at low Z values, and at intermediate values of $Z_{+/-}$, the aggregates reach neutrality that remains throughout the titration. This difference may be ascribed to the different PAm block sizes. For (PTEA)₉₆-*b*-(PEO)₁₀₀, the behavior is similar to the copolymers with smaller PAm blocks, where a more drastic charge inversion is observed.

Previous studies evaluated the effect of the blocks with respect to copolymers binding to DNA, focusing on keeping the neutral block length almost constant and varying the length of the cationic block. For example, the copolymer PMAG₅₂-*b*-PAEMA₆₃, where PAEMA is the cationic block, binds more strongly with DNA than PMAG₅₆-*b*-PAEMA₃₀, which was associated with a stronger interaction due to longer cationic block [25]. Those authors also suggest that even longer neutral blocks can limit the binding with DNA, impeding the interaction of the cationic moiety with the secondary structure of DNA assuming that hydrogen bonding does not effectively participate on the formation of the complexes [25]. In the present study, where the focus is on changing the neutral block length, clearly, this was not observed, and the initial aggregate size and the energetics of binding of different (PTEA)-*b*-(PAm) with DNA are similar. Changing the neutral block to PEO leads to a small increase in the binding affinity, as revealed by the thermodynamic functions reported in Table 2.

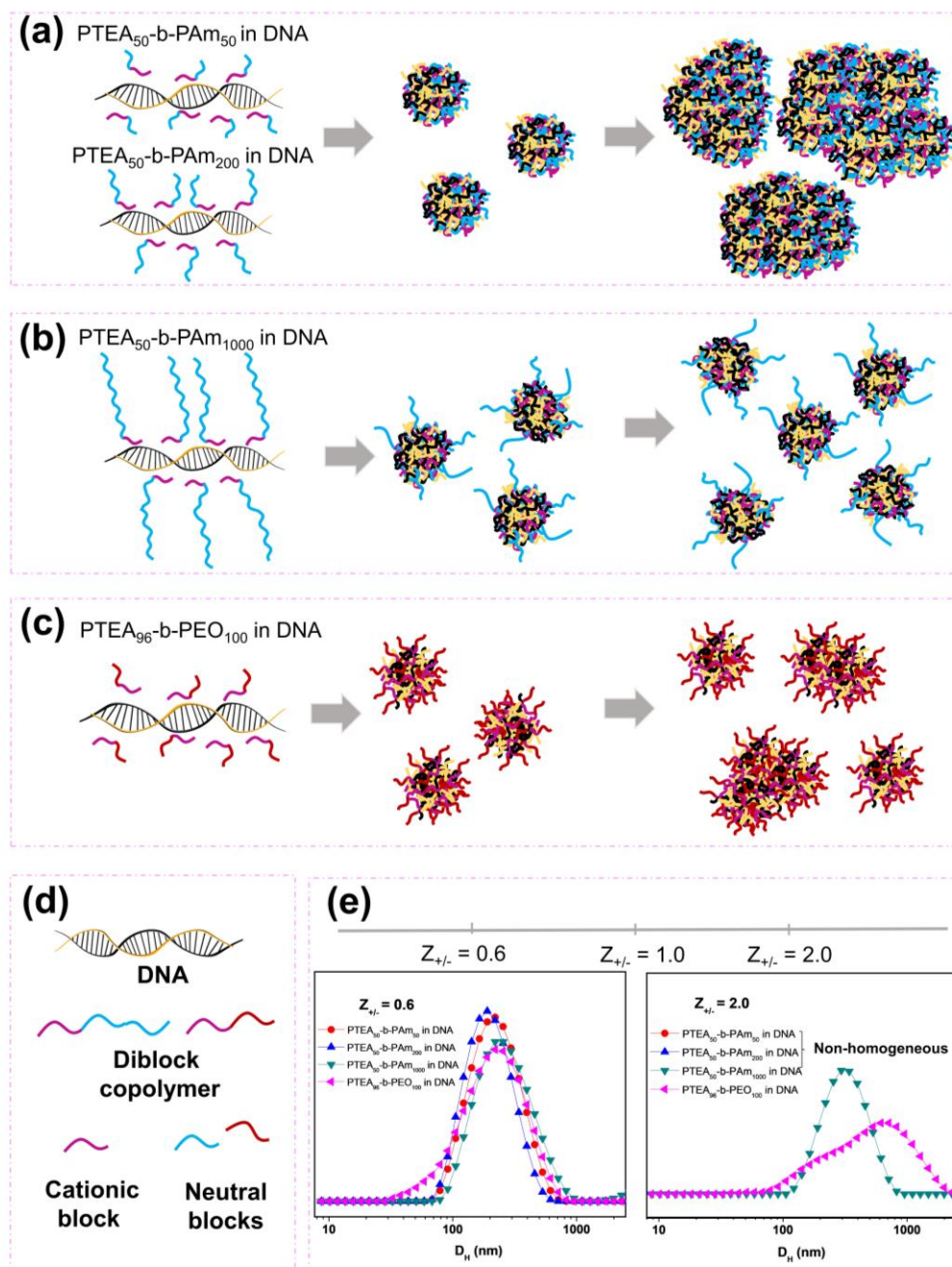


Figure 3. Illustration of the mechanism of interaction for the addition of (a) (PTEA)₅₀-b-(PAm)₅₀, (PTEA)₅₀-b-(PAm)₂₀₀, (b) (PTEA)₅₀-b-(PAm)₁₀₀₀, and (c) (PTEA)₉₆-b-(PEO)₁₀₀ into DNA solution. (d) Schematic representation of the macromolecules studied: (e) DLS results as a function of charge ratio, at $Z_{+/-} = 0.6$ and 2.0, for the polyplexes studied.

To evaluate the kinetic stability of the complexes, their sizes were monitored as function of time when formed upon direct mixture of the copolymers with DNA at $Z_{+/-} = 2.0$. As shown in Figure 4, the complex formed between (PTEA)₉₆-b-(PEO)₁₀₀ and DNA displays an initial size around 117 nm, and after 2 h, it slightly decreases to 112 nm, remaining constant up to 12 days. The size for the (PTEA)₅₀-b-(PAm)₅₀ and DNA complexes was initially of 130 nm and also presented a slight decrease to 120 nm and increased slightly to 155 nm after 12 days. Both complexes of DNA and (PTEA)₅₀-b-(PAm)₂₀₀ or (PTEA)₅₀-b-(PAm)₁₀₀₀ initially presented similar sizes, 141 and 146 nm, respectively. After 2 h, the (PTEA)₅₀-b-(PAm)₂₀₀ complex display a decrease on its size (121 nm), while

(PTEA)₅₀-*b*-(PAm)₁₀₀₀ and DNA complexes had a minor increase (152 nm). Interestingly, after 12 days, (PTEA)₅₀-*b*-(PAm)₁₀₀₀/DNA polyplexes decrease to 136 nm, almost the same size as (PTEA)₅₀-*b*-(PAm)₂₀₀/DNA polyplexes (140 nm). Overall, the size of aggregates at $Z_{+/-} = 2.0$ does not vary significantly within the investigation period.

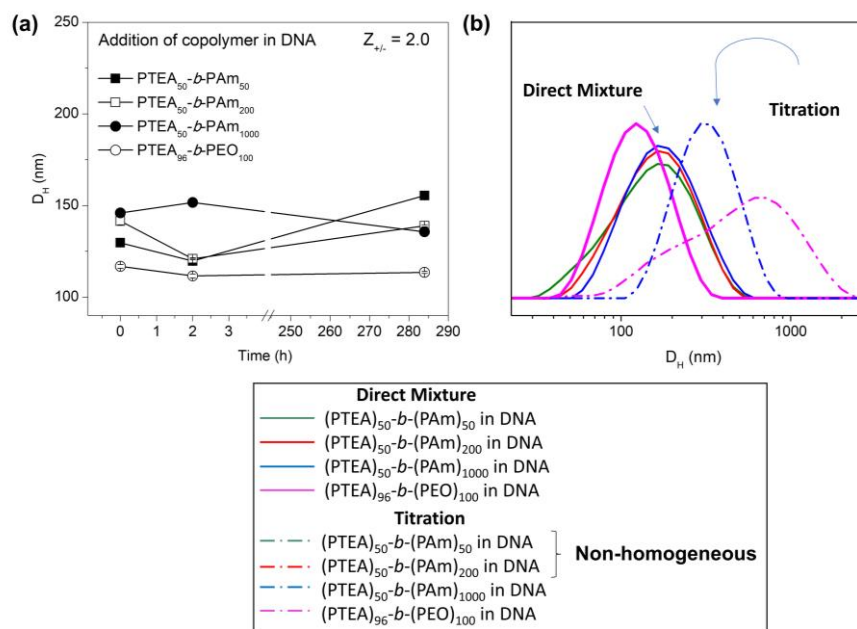


Figure 4. (a) Size of polyplexes prepared by direct mixture as function of time, with PDI values indicated as black bars and (b) size distribution of polyplexes obtained by direct mixture and titration, just after preparation.

However, when we assess the effect of their preparation protocol, either by continuous titration or via direct mixing, the difference in the polyplexes size is illustrated in Figure 4b. Using the direct mixture results in polyplexes significantly smaller compared to the titration protocol. Indeed, a previous study showed the direct mixture of DTAB with diblock copolymers (PAA)₅₀₀₀, g mol⁻¹-*b*-(PAm)_{30,000}, g mol⁻¹ generated aggregates smaller than those produced by the complex salt procedure [44].

Polyplexes were also prepared by titrating DNA into the copolymer solution in a reverse direction as previously used, and their sizes were compared to those prepared by titrating copolymer to DNA in Figure 5. As discussed before, the direct titration, that is, the addition of copolymers (PTEA)₅₀-*b*-(PAm)₅₀ and (PTEA)₅₀-*b*-(PAm)₂₀₀ into DNA (curves in black), led to precipitation at $Z_{+/-}$ approximately ≥ 1.0 , while (PTEA)₅₀-*b*-(PAm)₁₀₀₀ and (PTEA)₉₆-*b*-(PEO)₁₀₀ generated finite-sized structures. For the addition of DNA in the copolymers (red curves, reverse direction), at $Z_{+/-} \leq 1.0$ (excess of DNA), precipitation was observed except for (PTEA)₅₀-*b*-(PAm)₁₀₀₀. The delivery efficiency of a polyplex is improved whenever it possesses positive charge because it can interact with negatively charged cell membranes, and they are internalized to the cell via endocytosis [45]. After that, DNA must dissociate from the complexes to be released into the cytoplasm and conducted into the nucleus [45]. Polyplexes with approximately 200 nm displaying positive surface potential were obtained by adding DNA to all cationic copolymers. Upon the addition of (PTEA)₅₀-*b*-(PAm)₁₀₀₀ to DNA, it was possible to obtain polyplexes with positive surface potential; however, the size of the formed polyplexes was in the order of 400 nm, whereas polyplexes of around 200 nm were obtained when DNA was added to (PTEA)₅₀-*b*-(PAm)₁₀₀₀. This observation stresses the importance of selecting the preparation protocol for producing DNA polyplexes.

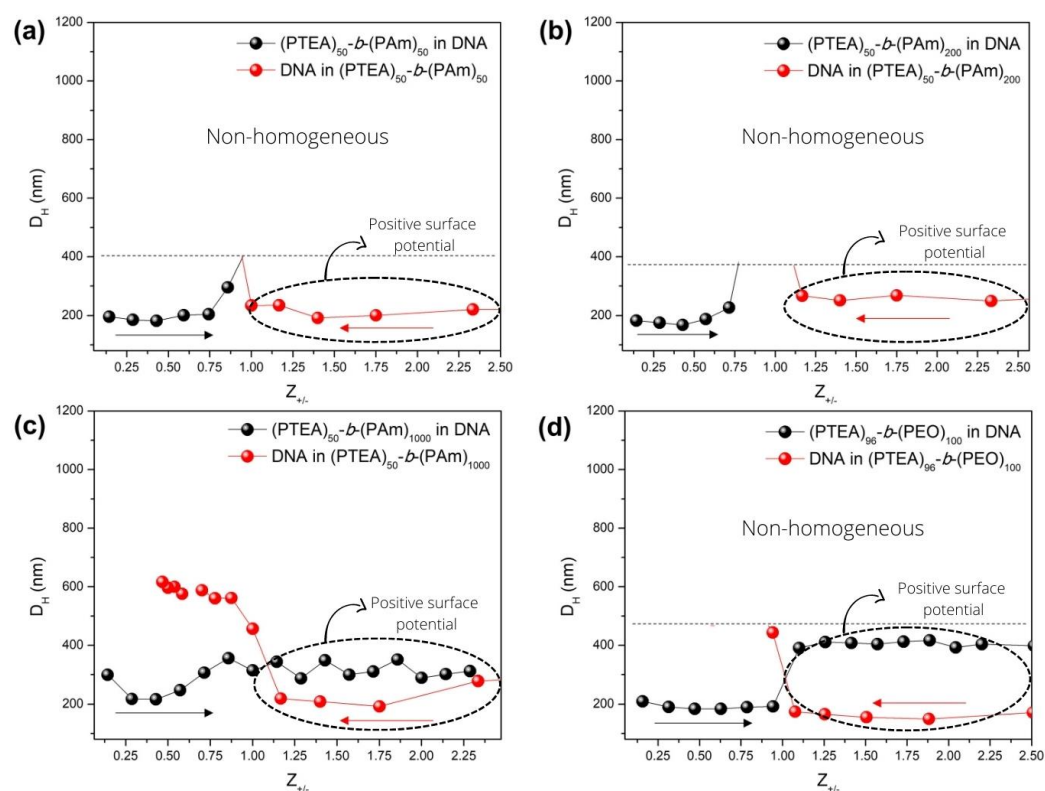


Figure 5. Size of polyplexes as function of charge ratio ($Z_{+/-}$) for the addition of (PTEA)₅₀-*b*-(PAm)₅₀ (a), (PTEA)₅₀-*b*-(PAm)₂₀₀ (b), (PTEA)₅₀-*b*-(PAm)₁₀₀₀ (c), and (PTEA)₉₆-*b*-(PEO)₁₀₀ (d) into DNA by direct addition (black) and addition of DNA into cationic block copolymer by reverse addition (red).

Circular dichroism (CD) was used to evaluate whether there were changes of DNA conformation induced by the addition of the cationic copolymers. The CD spectrum of DNA solution shows a positive band near 275 nm and a negative band close to 245 nm related to the stacking of DNA bases and to the helical structure of DNA, respectively (Figure 6). Upon addition of (PTEA)-*b*-(PAm), at $Z_{+/-} = 0.3$, the DNA secondary structure is not significantly affected independently of the copolymer although a red shift of the peak position is observed at $Z_{+/-} = 0.7$ and 1.5, which is similar to that observed in previous studies [25,46]. At $Z_{+/-} = 2.3$, there is no observable change on the DNA structure, which may indicate that the interaction is mainly electrostatic considering that hydrogen-bonding interaction is expected to modify the CD profile [20]. On the other hand, (PTEA)-*b*-(PEO)₁₀₀ induces changes in the DNA secondary structure in accordance with its strongest interactions with DNA, corroborating the previously discussed ITC results.

The CD results indicate that (PTEA)₉₆-*b*-(PEO)₁₀₀ displays the strongest binding to DNA, which can be ascribed to its longer cationic block. Other than that, the neutral block seems not to be interacting with DNA through hydrogen bonding between the acrylamide groups in the PAm block and the bases in the DNA. Indeed, Prevette and co-workers studied the condensation of DNA using a series of poly(glycoamidoamine)s and concluded that the binding mechanism is not only electrostatic but also through hydrogen bonding between the groups in the carbohydrate co-monomer and the DNA base pair [14]. Nevertheless, it has been suggested that this type of interaction occurs when the DNA chain is close to the groups that are capable of interacting through hydrogen bonding. When the blocks are separated, as in diblock copolymers, and the neutral block is not close to the cationic–anionic interaction sites [25], this type of interaction might not be so effective, as in the present study.

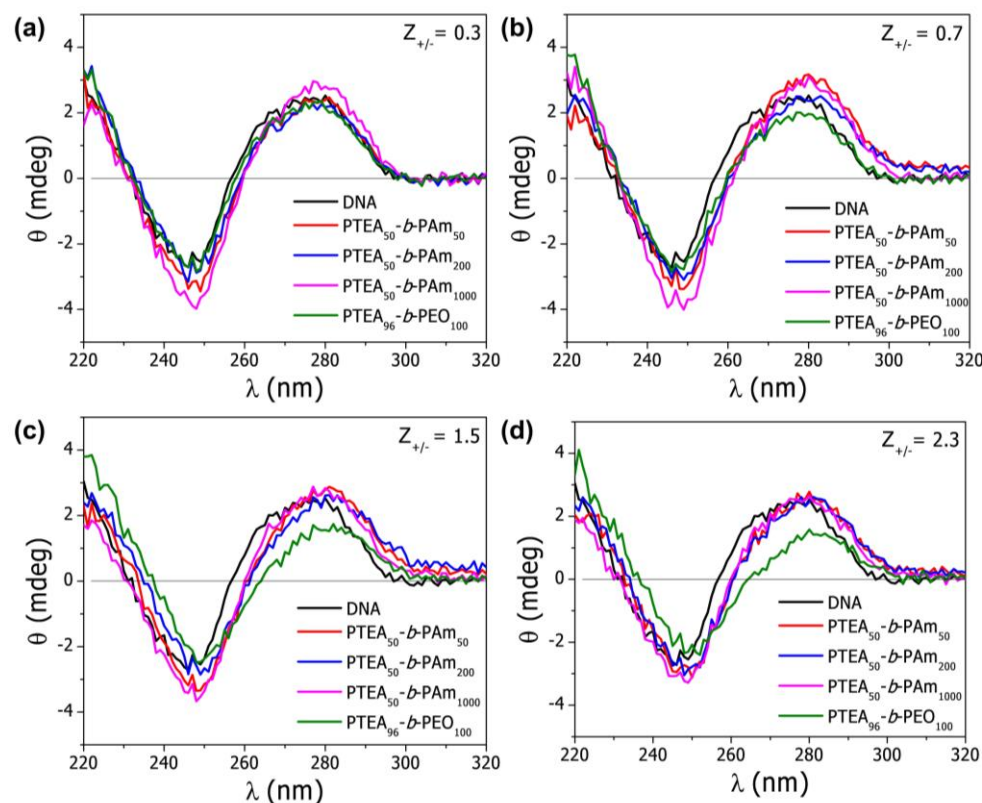


Figure 6. CD spectra of 0.4 mM DNA titrated with (PTEA)₅₀-*b*-(PAm)₅₀, (PTEA)₅₀-*b*-(PAm)₂₀₀, (PTEA)₅₀-*b*-(PAm)₁₀₀₀, or (PTEA)₉₆-*b*-(PEO)₁₀₀ with DNA at (a) $Z_{+/-} = 0.3$, (b) $Z_{+/-} = 0.7$, (c) $Z_{+/-} = 1.5$, and (d) $Z_{+/-} = 2.3$.

3. Materials and Methods

3.1. Materials

Salmon sperm DNA (2000 bp) was obtained from Sigma-Aldrich and used as received. Potassium ethyl xantogenate (purity 96%), methyl 2-bromopropionate (purity 98%), [2-(methacryloyloxy)ethyl] trimethyl ammonium chloride (TEA 80%), and 4,4'-Azobis(4-cyanovaleric acid) from Sigma-Aldrich were used without prior purification. Organic solvents methanol, hexane, ethyl acetate, isopropyl alcohol, acetone, ethyl ether, and 1,4-dioxane were purchased from Synth. Acrylamide (Am, Fluka, purity $\geq 98\%$) was recrystallized from methanol. The block copolymer (PTEA)-*b*-(PEO) was prepared as described below from poly(ethylene oxide)-*b*-poly(*n,n*-dimethylaminoethyl methacrylate), namely PEO-*b*-PDMAEMA, which was obtained from Polymer Source Inc., Dorval, QC, Canada, with M_n of 5000 g mol⁻¹-*b*-15000 g mol⁻¹. All other reagents were of the highest purity available and were used as received. Deionized water (Milli-Q, Millipore-18.2 M Ω cm) was used for all experiments.

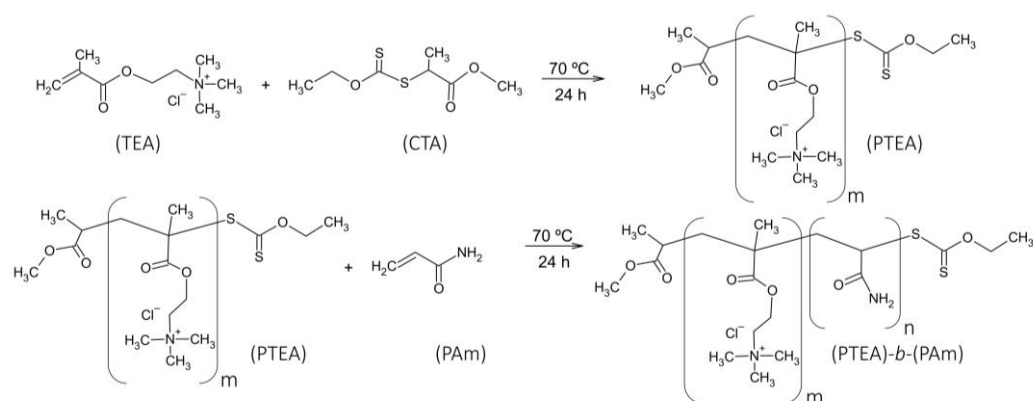
3.2. Block Copolymer Synthesis

3.2.1. Preparation of RAFT Agent (CTA)

The copolymers were prepared under argon atmosphere in a sealed flask by adding the RAFT agent (CTA), TEA, and initiator. The synthesis of S-(2-methylpropionate) O-ethyl xanthate (RAFT agent) was performed according to the methodology described in the literature [47], only using methanol as solvent instead of ethanol. The product was characterized by ¹H Nuclear Magnetic Resonance (¹H-NMR (250 MHz, CDCl₃): δ [ppm] = 4.63, 2H, q (C(S)OCH₂), 4.38, 1H, q (CH), 3.76, 3H, s (OCH₃), 1.58, 3H, d (CH₃) and 1.42, 3H, t (CH₃)).

3.2.2. Preparation of Homopolymer Poly(trimethyl-ammonium Chloride Metacrililoixietil) and Block Copolymers PTEA-*b*-PAm

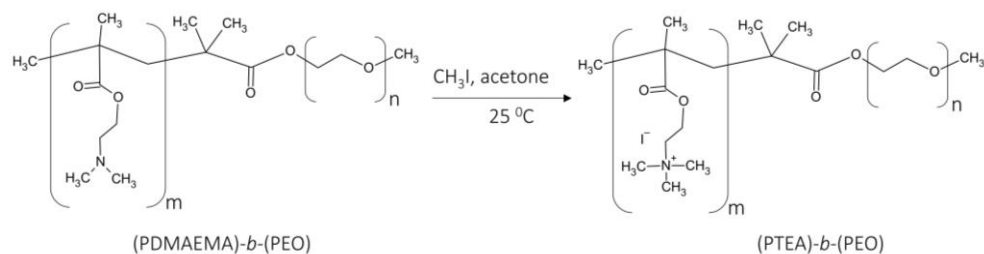
The block copolymers, poly(trimethyl-ammonium chloride metacrililoixietil)-*b*-poly(acrylamide) and (PTEA)_m-*b*-(PAm)_n (where m and n represent the degrees of polymerization of TEA and Am, respectively), were synthesized by Reversible Addition-Fragmentation chain Transfer (RAFT) using a xanthate as RAFT agent, following a methodology described in the literature [44,48] with some adaptations. The reactions were performed under argon atmosphere in a sealed flask by adding the transfer agent O-ethyl xanthate (CTA) and [2-(Methacryloyloxy)ethyl] trimethyl ammonium chloride (TEA) in a mixture of deionized water and isopropyl alcohol (4:1 *v/v*). Then, the initiator (4,4'-Azobis(4-cyanovaleric acid)) were added slowly dropwise, and the system reacted for 24 h at 70 °C (Scheme 2) [48]. For block copolymerization, acrylamide and initiator were added to the reaction and the solution left to react at 70 °C for 24 h. The copolymer was isolated from the solution by precipitation with an excess of 1,4-dioxane. Then, the copolymers were filtered and washed with 1,4-dioxane and dried at the room temperature using a vacuum [48]. The expected size of each block was defined in terms of the quantity of reactants used in the synthesis of (PTEA)-*b*-(PAm) [49], according to Table S1 (Supplementary Material).



Scheme 2. Schematic overview of the block copolymers preparation.

3.2.3. Modification of (PTEA)-*b*-(PEO)

To prepare (PTEA)-*b*-(PEO), the block copolymer (DMAEMA) was modified aiming at the quarternization of the tertiary amine groups according to the method described by Ranger and co-workers [50]. Briefly, the polymer (0.266 g) was added to a round-bottom flask with 10 mL of acetone. Then, 250 μ L of methyl iodide 99% was added. The solution was stirred during 16 h at 25 °C (Scheme 3). The resulting product was dialyzed against water and freeze-dried.



Scheme 3. Schematic overview of (PTEA)-*b*-(PEO) synthesis.

3.3. Polyplexes Preparation

Polyplexes were prepared by titrating the 4.0 mM block copolymer solution into a 0.4 mM DNA solution until the desired mole ratio ($Z_{+/-}$) was reached. Both solutions were prepared with 5.0 mM of NaCl. The pH of the solutions was not corrected since the

charges of the polyelectrolytes are expected to be independent of the pH medium. The polyplexes were also prepared by titrating a 4.0 mM DNA solution into a 0.4 mM block copolymer solution. Further experiments were performed by adding block copolymer into DNA solution in one step to achieve the charge ratio ($Z_{+/-}$) of 2.0, and the complexes' sizes were monitored as a function of time. During this period of time, the complexes formed were stored at 25 °C.

3.4. Isothermal Titration Calorimetry

Titration of (PTEA)-*b*-(PEO) or (PTEA)-*b*-(PAm) with DNA solutions were performed to investigate the energetics of binding. ITC experiments were performed in a VP-ITC (MicroCal, Amherst, MA, USA) isothermal titration calorimeter with a sample cell of 1.43 mL. A more concentrated solution (4.0 mM) of polymer was consecutively injected with a gastight syringe that also acted as a stirrer (at 329 rpm) into a solution at 0.4 mM of DNA in the cell. This concentration was calculated considering the molar composition in terms of charge equivalents (for this system, one charge equals one mer). Injection volumes varied between 10 and 15 μ L with an interval of 800 s between each injection. The volume of the cell was kept constant during the experiments due to an overflow of solution, and this was considered during calculations of the actual cell concentrations. Polymer and DNA dilution heat effects were determined and found to be negligible.

3.5. Dynamic Light-Scattering and Zeta Potential Measurements

Dynamic light-scattering and zeta potential measurements were performed with a Malvern Instruments Autosizer model 4700, UK. The hydrodynamic diameter (D_H) of the polyplexes was expressed by means of their Z-average. These polyplexes were obtained by titrating copolymer into DNA solution or vice versa and by direct mixture at a specific charge ratio. The electrophoretic mobility of the samples was determined from the average of 15 cycles of an applied electric field. Their zeta potential was determined from their electrophoretic mobility using the Smoluchowski approximation.

3.6. Circular Dichroism (CD)

CD spectra of the polyplexes were obtained using a Jasco 715, Japan, spectropolarimeter to monitor the conformation of DNA in the polyplexes. The spectral range varied from 220–320 nm with a scan rate of 20 nm·min⁻¹, and the reported spectra are an average of three accumulations. The samples were maintained at 25 °C in a 1 mm pathlength quartz cuvette. To prepare the polyplexes, a DNA solution of 0.4 mM was used and titrated with a 4.0 mM polymer solution until the desired charge ratio.

4. Conclusions

Four different block copolymers were used with the same cationic block in order to compare the influence of the nature and length of the neutral block on their interaction with salmon sperm DNA. Calorimetric measurements showed that the interaction is endothermic, around 4.0 kJ mol⁻¹ of charges for the copolymers (PTEA)-*b*-(PAm) and around 5.5 kJ mol⁻¹ of charges for (PTEA)₉₆-*b*-(PEO)₁₀₀, indicating that the formation of the complex is entropically driven, probably due to the release of counterions and water molecules. For all copolymers, the enthalpy change is constant up to a critical charge ratio ($Z_{+/-}$) of about 0.8 for the addition of polymer to DNA. These calorimetric measurements also confirm that the polyplex formation is a two-step process including an ion-pairing and a coacervation stages.

The complexes hydrodynamic diameter was determined by DLS as around 200 nm before $Z_{+/-}$ approximately 1.0. After charge neutrality, precipitation occurred for the complexes of (PTEA)₅₀-*b*-(PAm)₅₀ and (PTEA)₅₀-*b*-(PAm)₂₀₀ and DNA, whereas the size of polyplexes of DNA and (PTEA)₅₀-*b*-(PAm)₁₀₀₀ remained almost constant even at high $Z_{+/-}$. The polyplexes of (PTEA)₉₆-*b*-(PEO)₁₀₀ and DNA display diameters around 200 nm at $Z_{+/-} = 0.6$, and after charge neutrality was reached, a broad size distribution was observed.

Interestingly, for all the copolymers studied, the complexes prepared by direct mixture at $Z_{+/-} = 2.0$ were smaller than those prepared by titration, indicating that the protocol of preparation affects the polyplexes formation. Varying the order of addition, that is, performing the titration of copolymer into DNA or vice versa (direct or reverse titration, respectively), was found to affect both the size and charge of the polyplexes, and this can be used to modulate the characteristics of polyplexes for varied applications.

Supplementary Materials: The following supporting information can be downloaded at: <https://www.mdpi.com/article/10.3390/molecules28010398/s1>, Figure S1: Gel permeation chromatograms obtained for the copolymers (PTEA)₅₀-b-(PAm)₅₀, (PTEA)₅₀-b-(PAm)₂₀₀, and (PTEA)₅₀-b-(PAm)₁₀₀₀; Table S1: Mass of reactants used in the synthesis of copolymers (PTEA)₅₀-b-(PAm)₅₀, (PTEA)₅₀-b-(PAm)₂₀₀, and (PTEA)₅₀-b-(PAm)₁₀₀₀ [49].

Author Contributions: Conceptualization, R.M.G., L.V. and W.L.; methodology, R.M.G., L.V. and W.L.; validation R.M.G., L.V. and W.L.; investigation, R.M.G. and L.V.; resources, W.L.; writing—original draft preparation, R.M.G. and L.V.; writing—review and editing, R.M.G., L.V. and W.L.; supervision, W.L.; project administration, W.L. and R.M.G.; funding acquisition, W.L. All authors have read and agreed to the published version of the manuscript.

Funding: This research was funded by FAPESP through thematic projects 2015/25406-5 and 2021/12071-6 and through a postdoctoral grant to RMG (10/00528-7).

Data Availability Statement: The data presented in this study are available on request from the corresponding author.

Acknowledgments: The authors would like to acknowledge FAPESP for the financial support through thematic projects 2015/25406-5 and 2021/12071-6 and through a postdoctoral grant to RMG (10/00528-7). We thank INCT-Catálise, Marcos Vinicius Aquino Queirós, Guilherme C. Campese, Professor José Adilson de Castro, and Professor Karin Schillén for helpful discussions. We would like to dedicate this article to Professor Bjorn Lindman on the occasion of his 80th birthday. We acknowledge him as a role model as a scientist, for his many important contributions to Colloid Science, and for his interest in and support for our research activities.

Conflicts of Interest: The authors declare no conflict of interest.

Sample Availability: Samples of the compounds are available from the authors.

References

1. Chen, X.M.; Feng, W.J.; Bisoyi, H.K.; Zhang, S.; Chen, X.; Yang, H.; Li, Q. Light-Activated Photodeformable Supramolecular Dissipative Self-Assemblies. *Nat. Commun.* **2022**, *13*, 3216. [CrossRef] [PubMed]
2. Chen, X.M.; Hou, X.F.; Bisoyi, H.K.; Feng, W.J.; Cao, Q.; Huang, S.; Yang, H.; Chen, D.; Li, Q. Light-Fueled Transient Supramolecular Assemblies in Water as Fluorescence Modulators. *Nat. Commun.* **2021**, *12*, 4993. [CrossRef] [PubMed]
3. Huang, D.; Korolev, N.; Eom, K.D.; Tam, J.P.; Nordenskiöld, L. Design and Biophysical Characterization of Novel Polycationic E-Peptides for DNA Compaction and Delivery. *Biomacromolecules* **2008**, *9*, 321–330. [CrossRef] [PubMed]
4. Nisha, C.K.; Manorama, S.V.; Ganguli, M.; Maiti, S.; Kizhakkedathu, J.N. Complexes of Poly(Ethylene Glycol)-Based Cationic Random Copolymer and Calf Thymus DNA: A Complete Biophysical Characterization. *Langmuir* **2004**, *20*, 2386–2396. [CrossRef] [PubMed]
5. Insua, I.; Wilkinson, A.; Fernandez-Trillo, F. Polyion Complex (PIC) Particles: Preparation and Biomedical Applications. *Eur. Polym. J.* **2016**, *81*, 198–215. [CrossRef] [PubMed]
6. St. John, P.M.; Westervelt, K.; Rimawi, A.; Kawakita, T. Binding between an Amine Cationic Surfactant and DNA and Surface Properties of the Resultant Aggregates. *Biophys. Chem.* **2022**, *281*, 106734. [CrossRef]
7. Barreleiro, P.C.A.; Olofsson, G.; Alexandridis, P. Interaction of DNA with Cationic Vesicles: A Calorimetric Study. *J. Phys. Chem. B* **2000**, *104*, 7795–7802. [CrossRef]
8. Akram, M.; Lal, H. Kabir-ud-Din Exploring the Binding Mode of Ester-Based Cationic Gemini Surfactants with Calf Thymus DNA: A Detailed Physicochemical, Spectroscopic and Theoretical Study. *Bioorg. Chem.* **2022**, *119*, 105555. [CrossRef]
9. Petersen, H.; Kunath, K.; Martin, A.L.; Stolnik, S.; Roberts, C.J.; Davies, M.C.; Kissel, T. Star-Shaped Poly(Ethylene Glycol)-Block-Polyethylenimine Copolymers Enhance DNA Condensation of Low Molecular Weight Polyethylenimines. *Biomacromolecules* **2002**, *3*, 926–936. [CrossRef]
10. Bellettini, I.C.; Fayad, S.J.; Machado, V.G.; Minatti, E. Properties of Polyplexes Formed through Interaction between Hydrophobically-Modified Poly(Ethylene Imine)s and Calf Thymus DNA in Aqueous Solution. *Soft Matter* **2017**, *13*, 2609–2619. [CrossRef]

11. Sabín, J.; Alatorre-Meda, M.; Miñones, J.; Domínguez-Arca, V.; Prieto, G. New Insights on the Mechanism of Polyethylenimine Transfection and Their Implications on Gene Therapy and DNA Vaccines. *Colloids Surf. B Biointerfaces* **2021**, *210*, 112219. [[CrossRef](#)] [[PubMed](#)]
12. Eldred, S.E.; Pancost, M.R.; Otte, K.M.; Rozema, D.; Stahl, S.S.; Gellman, S.H. Effects of Side Chain Configuration and Backbone Spacing on the Gene Delivery Properties of Lysine-Derived Cationic Polymers. *Bioconjugate Chem.* **2005**, *16*, 694–699. [[CrossRef](#)] [[PubMed](#)]
13. Veleva-kostadinova, E.; Dimitrov, I.; Toncheva-moncheva, N.; Novakov, C.; Momekova, D.; Rangelov, S. Nanoparticulate Polyelectrolyte Complexes of Thermally Sensitive Poly(L-Lysine)-Based Copolymers and DNA. *Eur. Polym. J.* **2018**, *102*, 219–230. [[CrossRef](#)]
14. Prevette, L.E.; Kodger, T.E.; Reineke, T.M.; Lynch, M.L. Deciphering the Role of Hydrogen Bonding in Enhancing PDNA-Polycation Interactions. *Langmuir* **2007**, *23*, 9773–9784. [[CrossRef](#)]
15. Molina-pinilla, I.; Hakkou, K.; Romero-azogil, L.; Benito, E.; García-martín, M.G.; Bueno-martínez, M. Synthesis of Degradable Linear Cationic Poly(Amide Triazole)s with DNA-Condensation Capability. *Eur. Polym. J.* **2019**, *113*, 36–46. [[CrossRef](#)]
16. Braun, C.S.; Vetro, J.A.; Tomalia, D.A.; Koe, G.S.; Koe, J.G.; Middaugh, C.R. Structure/Function Relationships of Polyamidoamine/DNA Dendrimers as Gene Delivery Vehicles. *J. Pharm. Sci.* **2005**, *94*, 423–436. [[CrossRef](#)]
17. Öberg, M.-L.; Schillén, K.; Nylander, T. Dynamic Light Scattering and Fluorescence Study of the Interaction between Double-Stranded DNA and Poly (Amido Amine) Dendrimers. *Biomacromolecules* **2007**, *8*, 1557–1563. [[CrossRef](#)]
18. Cárdenas, M.; Schillén, K.; Pebalk, D.; Nylander, T.; Lindman, B. Interaction between DNA and Charged Colloids Could Be Hydrophobically Driven. *Biomacromolecules* **2005**, *6*, 832–837. [[CrossRef](#)]
19. Franck, C.O.; Fanslau, L.; Popov, A.B.; Tyagi, P.; Fruk, L. Biopolymer-Based Carriers for DNA Vaccine Design. *Angew. Chem. Int. Ed.* **2021**, *60*, 13225–13243. [[CrossRef](#)]
20. Albuquerque, L.J.C.; Annes, K.; Milazzotto, M.P.; Mattei, B.; Riske, K.A.; Jäger, E.; Pánek, J.; Štěpánek, P.; Kapusta, P.; Muraro, P.I.R.; et al. Efficient Condensation of DNA into Environmentally Responsive Polyplexes Produced from Block Cationomers Carrying Amine or Diamine Groups. *Langmuir* **2016**, *32*, 577–586. [[CrossRef](#)]
21. Jung, S.; Lodge, T.P.; Reineke, T.M. Structures and Protonation States of Hydrophilic–Cationic Diblock Copolymers and Their Binding with Plasmid DNA. *J. Phys. Chem. B* **2018**, *122*, 2449–2461. [[CrossRef](#)] [[PubMed](#)]
22. Chen, B.; Yu, L.; Li, Z.; Wu, C. Design of Free Triblock Polylysine-b-Polyleucine-b-Polylysine Chains for Gene Delivery. *Biomacromolecules* **2018**, *19*, 1347–1357. [[CrossRef](#)] [[PubMed](#)]
23. Funhoff, A.M.; Van Nostrum, C.F.; Lok, M.C.; Fretz, M.M.; Crommelin, D.J.A.; Hennink, W.E. Poly(3-Guanidinopropyl Methacrylate): A Novel Cationic Polymer for Gene Delivery. *Bioconjugate Chem.* **2004**, *15*, 1212–1220. [[CrossRef](#)] [[PubMed](#)]
24. Nimesh, S.; Chandra, R. Guanidinium-Grafted Polyethylenimine: An Efficient Transfecting Agent for Mammalian Cells. *Eur. J. Pharm. Biopharm.* **2008**, *68*, 647–655. [[CrossRef](#)] [[PubMed](#)]
25. Jung, S.; Lodge, T.P.; Reineke, T.M. Complexation between DNA and Hydrophilic–Cationic Diblock Copolymers. *J. Phys. Chem. B* **2017**, *121*, 2230–2243. [[CrossRef](#)]
26. Alatorre-Meda, M.; Taboada, P.; Krajewska, B.; Willemeit, M.; Deml, A.; Klösel, R.; Rodríguez, J.R. DNA-Poly(Diallyldimethylammonium Chloride) Complexation and Transfection Efficiency. *J. Phys. Chem. B* **2010**, *114*, 9356–9366. [[CrossRef](#)]
27. Haladjova, E.; Mountrichas, G.; Pispas, S.; Rangelov, S. Poly(Vinyl Benzyl Trimethylammonium Chloride) Homo and Block Copolymers Complexation with DNA. *J. Phys. Chem. B* **2016**, *120*, 2586–2595. [[CrossRef](#)]
28. Sharma, R.; Lee, J.S.; Bettencourt, R.C.; Xiao, C.; Konieczny, S.F.; Won, Y.Y. Effects of the Incorporation of a Hydrophobic Middle Block into a PEG-Polycation Diblock Copolymer on the Physicochemical and Cell Interaction Properties of the Polymer-DNA Complexes. *Biomacromolecules* **2008**, *9*, 3294–3307. [[CrossRef](#)]
29. Knaapila, M.; Costa, T.; Garamus, V.M.; Kraft, M.; Drechsler, M.; Scherf, U.; Burrows, H.D. Polyelectrolyte Complexes of a Cationic All Conjugated Fluorene-Thiophene Diblock Copolymer with Aqueous DNA. *J. Phys. Chem. B* **2015**, *119*, 3231–3241. [[CrossRef](#)]
30. Dootz, R.; Toma, A.C.; Pfohl, T. PAMAM6 Dendrimers and DNA: PH Dependent “Beads-on-a-String” Behavior Revealed by Small Angle X-Ray Scattering. *Soft Matter* **2011**, *7*, 8343–8351. [[CrossRef](#)]
31. Jiang, Y.; Reineke, T.M.; Lodge, T.P. Complexation of DNA with Cationic Copolymer Micelles: Effects of DNA Length and Topology. *Macromolecules* **2018**, *51*, 1150–1160. [[CrossRef](#)]
32. Ping, Y.; Ding, D.; Ramos, R.A.N.S.; Mohanram, H.; Deepankumar, K.; Gao, J.; Tang, G.; Miserez, A. Supramolecular β -Sheets Stabilized Protein Nanocarriers for Drug Delivery and Gene Transfection. *ACS Nano* **2017**, *11*, 4528–4541. [[CrossRef](#)] [[PubMed](#)]
33. Pandey, A.P.; Sawant, K.K. Polyethylenimine: A Versatile, Multifunctional Non-Viral Vector for Nucleic Acid Delivery. *Mater. Sci. Eng. C* **2016**, *68*, 904–918. [[CrossRef](#)] [[PubMed](#)]
34. Alvarez-Lorenzo, C.; Barreiro-Iglesias, R.; Concheiro, A.; Iourtchenko, L.; Alakhov, V.; Bromberg, L.; Temchenko, M.; Deshmukh, S.; Hatton, T.A. Biophysical Characterization of Complexation of DNA with Block Copolymers of Poly(2-Dimethylaminoethyl) Methacrylate, Poly(Ethylene Oxide), and Poly(Propylene Oxide). *Langmuir* **2005**, *21*, 5142–5148. [[CrossRef](#)]
35. Herrera, I.; Winnik, M.A. Differential Binding Models for Isothermal Titration Calorimetry: Moving beyond the Wiseman Isotherm. *J. Phys. Chem. B* **2013**, *117*, 8659–8672. [[CrossRef](#)] [[PubMed](#)]
36. Lounis, F.M.; Chamieh, J.; Leclercq, L.; Gonzalez, P.; Geneste, A.; Prelot, B.; Cottet, H. Interactions between Oppositely Charged Polyelectrolytes by Isothermal Titration Calorimetry: Effect of Ionic Strength and Charge Density. *J. Phys. Chem. B* **2017**, *121*, 2684–2694. [[CrossRef](#)]

37. Olofsson, G.; Loh, W. On the Use of Titration Calorimetry to Study the Association of Surfactants in Aqueous Solutions. *J. Braz. Chem. Soc.* **2009**, *20*, 577–593. [[CrossRef](#)]
38. Vitorazi, L.; Ould-Moussa, N.; Sekar, S.; Fresnais, J.; Loh, W.; Chapel, J.P.; Berret, J.F. Evidence of a Two-Step Process and Pathway Dependency in the Thermodynamics of Poly(Diallyldimethylammonium Chloride)/Poly(Sodium Acrylate) Complexation. *Soft Matter* **2014**, *10*, 9496–9505. [[CrossRef](#)]
39. Cingil, H.E.; Boz, E.B.; Wang, J.; Stuart, M.A.C.; Sprakel, J. Probing Nanoscale Coassembly with Dual Mechanochromic Sensors. *Adv. Funct. Mater.* **2016**, *26*, 1420–1427. [[CrossRef](#)]
40. Priftis, D.; Laugel, N.; Tirrell, M. Thermodynamic Characterization of Polypeptide Complex Coacervation. *Langmuir* **2012**, *28*, 15947–15957. [[CrossRef](#)]
41. Skandalis, A.; Uchman, M.; Štěpánek, M.; Kerelche, S.; Pispas, S. Complexation of DNA with QPDMAEMA-b-PLMA-b-POEGMA Cationic Triblock Terpolymer Micelles. *Macromolecules* **2020**. [[CrossRef](#)]
42. Matulis, D.; Rouzina, I.; Bloomfield, V.A. Thermodynamics of DNA Binding and Condensation: Isothermal Titration Calorimetry and Electrostatic Mechanism. *J. Mol. Biol.* **2000**, *296*, 1053–1063. [[CrossRef](#)] [[PubMed](#)]
43. Kim, W.; Yamasaki, Y.; Kataoka, K. Development of a Fitting Model Suitable for the Isothermal Titration Calorimetric Curve of DNA with Cationic Ligands. *J. Phys. Chem. B* **2006**, *110*, 10919–10925. [[CrossRef](#)] [[PubMed](#)]
44. Vitorazi, L.; Berret, J.F.; Loh, W. Self-Assembly of Complex Salts of Cationic Surfactants and Anionic-Neutral Block Copolymers. Dispersions with Liquid-Crystalline Internal Structure. *Langmuir* **2013**, *29*, 14024–14033. [[CrossRef](#)]
45. Machtakova, M.; Thérien-Aubin, H.; Landfester, K. Polymer Nano-Systems for the Encapsulation and Delivery of Active Biomacromolecular Therapeutic Agents. *Chem. Soc. Rev.* **2022**, *51*, 128–152. [[CrossRef](#)]
46. Maruyama, A.; Watanabe, H.; Ferdous, A.; Katoh, M.; Ishihara, T.; Akaike, T. Characterization of Interpolyelectrolyte Complexes between Double-Stranded DNA and Polylysine Comb-Type Copolymers Having Hydrophilic Side Chains. *Bioconjugate Chem.* **1998**, *9*, 292–299. [[CrossRef](#)]
47. Pound, G.; Eksteen, Z.; Pfukwa, R.; McKenzie, J.M.; Lange, R.F.M.; Klumperman, B. Unexpected Reactions Associated with the Xanthate-Mediated Polymerization of N-Vinylpyrrolidone. *J. Polym. Sci. Part A. Polym. Chem.* **2008**, *46*, 6575–6593. [[CrossRef](#)]
48. Taton, D.; Wilczewska, A.Z.; Destarac, M. Direct Synthesis of Double Hydrophilic Statistical Di- and Triblock Copolymers Comprised of Acrylamide and Acrylic Acid Units via the MADIX Process. *Macromol. Rapid Commun.* **2001**, *22*, 1497–1503. [[CrossRef](#)]
49. Lowe, A.B.; McCormick, C.L. Reversible Addition-Fragmentation Chain Transfer (RAFT) Radical Polymerization and the Synthesis of Water-Soluble (Co)Polymers under Homogeneous Conditions in Organic and Aqueous Media. *Prog. Polym. Sci.* **2007**, *32*, 283–351. [[CrossRef](#)]
50. Ranger, M.; Jones, M.; Yessine, M.-A.; Leroux, J.-C. From Well-Defined Diblock Copolymers Prepared by a Versatile Atom Transfer Radical Polymerization Method to Supramolecular Assemblies. *J. Polym. Sci. A Polym. Chem.* **2001**, *39*, 3861–3874. [[CrossRef](#)]

Disclaimer/Publisher's Note: The statements, opinions and data contained in all publications are solely those of the individual author(s) and contributor(s) and not of MDPI and/or the editor(s). MDPI and/or the editor(s) disclaim responsibility for any injury to people or property resulting from any ideas, methods, instructions or products referred to in the content.